Korean J. Chem. Eng., 32(6), 1101-1118 (2015)
DOI: 10.1007/s11814-014-0310-1

pISSN: 0256-1115
eISSN: 1975-7220

Experimental investigation and modeling of industrial oily wastewater treatment using modified polyethersulfone ultrafiltration hollow fiber membranes

Abdolhamid Salahi*, Toraj Mohammadi*, Reza Mosayebi Behbahani,†, and Mahmood Hemmati*****

*Research Centre for Membrane Separation Processes (RCMSP), Faculty of Chemical Engineering, Iran University of Science and Technology (IUST), Narmak, Tehran 16846, Iran
**Department of Gas & Chemical Engineering, Petroleum University of Technology (PUT), Ahwaz, Iran
***Polymer Science and Technology Division, Research Institute of Petroleum Industry, West Blvd., Near Azadi Sports Complex, Tehran, Iran
(*Received 16 August 2014 • accepted 9 October 2014*)

Abstract−Hollow fiber membranes were prepared from polyethersulfone/additives/NMP&DMSO system via phase inversion induced by precipitation in non-solvent coagulation bath. The interaction effects of polyethylene-glycol (PEG), propionic-acid (PA), Tween-20, PEG molecular weight and polyvinyl-pyrrolidone (PVP) on morphology and performance of synthesized membranes were investigated. Taguchi method (L_{16} orthogonal array) was used initially to plan a minimum number of experiments. 32 membranes were synthesized (with two replications) and their permeation flux and TOC rejection properties to oily wastewater treatment were studied. The obtained results indicated that addition of PA to spinning dope decreases flux while it increases TOC rejection of prepared membranes. Also, the result shows that addition of PVP, Tween-20 and PEG content in spinning dope enhances permeation flux while reducing TOC rejection. The obtained results indicated that the synthesized membranes was effective and suitable for treatment of the oily wastewater to achieve up to 92.6, 98.2, and 98.5% removal of TOC, TSS, and OGC, respectively with a flux of 247.19 L/(m^2h). Moreover, Hermia's models were used for permeation flux decline prediction. Experimental data and models predictions were compared. The results showed that there is reasonable agreement between experimental data and the cake layer model followed by the intermediate blocking model.

Keywords: Oily Wastewater, Hollow Fiber Membranes, Non-solvent Additive, Morphology, Taguchi Method, Modeling

INTRODUCTION

The generation of oily industrial wastewater and oil in waters has been recognized as one of the most concerned pollution causes. The discharge of oily wastewater into the natural environment creates a major ecological problem throughout the world [1,2]. For example, oily industrial wastewater in Iranian industries (e.g. Tehran Oil Refining Company) involves over 100 plants discharging over 1,000 m^3/day each [3]. Main industrial sources of this wastewater include oil refineries, oil distribution, petrochemical complexes, food producers, textiles, machining factories and metal manufacturing. The wastewater has large amounts of cutting liquids, total suspended solids (TSS), lubricants, light naphtha (liquefied petroleum gas, jet fuel, kerosene and gasoline), heavy naphtha (fuel oil, lube cut, grease and diesel oil). The Canadian and European regulations, according to the new guidelines, require treated oily wastewater to have less than 5 ppm oil content before being discharged into the environment [3,4].

Traditional treatment processes which consist of API (American Petroleum Institute) separator, gravity separation and skimming, emulsion breaking, dissolved air flotation, de-emulsion coagulation and flocculation, aeration zone and settler are often costly and ineffective [5-7]. Gravity separation and API separator methods followed by skimming is effective in removing free oil from oily industrial wastewater [3]. Overall, all these conventional methods are not sufficient to achieve the water quality requirement needed for recycling wastewaters such as are disposed into the environment or reused as agricultural water. Also, they are highly energy intensive, and hence, very expensive [2,8]. One of the treatment techniques used for oil separation from industrial wastewater is membrane filtration [3,9].

Membrane technology in wastewater treatment has made significant progress in recent years. Several studies have reported on the effectiveness of membrane processes in treating oily wastewaters [2,9-11]. Unstable oil is removed easily by microfiltration (MF) membranes, but dissolved oil passes the MF membrane pores so that removal efficiency of this process is not satisfactory [3,12]. Previous experimental investigations indicated that treatment of these wastewaters using MF does not satisfy the environmental standards. Ultrafiltration (UF) has been found to be an effective method for treatment of oily wastewater and many researchers have reported on its efficiency and effectiveness [2,13].

Microporous membrane processes like microfiltration (MF) and ultrafiltration (UF) are employed to separate micro-solutes from macromolecules and to industrial wastewater treatment and water reuse. A wide range of polymeric materials can be utilized for micro-

†To whom correspondence should be addressed.
E-mail: rezabehbahaniput@gmail.com, salahi@iust.ac.ir

porous membrane fabrication, such as polysulfone (PSf), polyethersulfone (PES), polyacrilonitrile (PAN), and polyvinylidine fluoride (PVDF). All polymers can be applied as membrane materials, but their physiochemical, rheological properties and chemical resistance differ so much that only a limited number are used in industrial and laboratory applications. PES is regarded as one of the most attractive polymer materials in the microporous membrane industry and is employed in water reuse, wastewater treatment, hemodialysis, metallurgy, milk industries, petrochemicals, etc. This polymer is widely used for fabrication of MF, UF, pervaporation (PV) and gas separation (GS) membranes. It provides easy preparation in a wide variety of configurations and modules, has extraordinary mechanical properties, wide range of pore sizes available for UF and MF applications ranging from 1.0 nm to 0.2 μm, high chemical resistance, good thermal stability (wide operating temperature limits), fairly good chlorine resistance and excellent membrane forming abilities [14,15]. Thus, PES is a suitable material to make membranes which have been applied in oil in water reuse and oily wastewater treatment.

Membrane morphology has an important influence on improving permeability and rejection. High rejections are usually accompanied by low permeabilities. During preparation, the membrane formation process plays a main role and certain factors need proper attention in order to produce a good performance membrane. The extensive experimental results show that the controllable factors play an important role in the membrane formation mechanism and consequently the hollow fiber membrane morphology and permeability, such as concentration of polymer in the dope solution [16], evaporation time [17], type of solvent/non-solvent pair [18], cast film thickness [19], air-gap distance [18], choosing non-solvent/solvent pairs with low mutual affinity [20], take-up speed [18], presence of certain additives [21], addition of solvent to the coagulation bath [22], coagulation bath temperature (CBT) [23], presence of some other solvents [24], and addition of non-solvent to the polymer solution [25,26]. It shows that the above parameters have important influences on the membrane morphology in the coagulation bath during the membrane formation process. Polymer additives such as PA, PVP, Tween-20 and PEG have been widely used to control the membrane structure in preparation of UF and MF membranes. To reduce the fouling tendency of these membranes, their wettability should be improved and their biocompatibility enhanced by adding hydrophilic polymeric additives such as PVP and PEG [27,28]. Recently, Amirilargani and Mohammadi [29] investigated the influence of propionic acid (PA) in the dope on morphology and performance of polyethersulfone (PES) membranes. They realized that permeation flux decreases and rejection increases by increasing of PA additives in the dope. Wienk et al. studied the effects of addition of high and low molecular weight (MW) components to the dope and proposed a mechanism for the formation of finger-like structures in the membrane top layer [30]. Idris et al. [31] investigated that the presence of PEG with different MWs indicates considerable effects on the performance of PES membranes. They discovered that the presence of PEG 400 and PEG 600 in the dope and increasing their concentration increases permeation flux but decreases rejection. Contradictory results were reported for PEG 200 by Idris et al. [31]: addition of PEG 200 to the dope leads to lower permeation fluxes, while higher rejections. There are several mechanisms by which such additives can affect the final membrane morphology and permeability. The effect of PVP as a polymeric additive on permeability properties and morphology of polymeric membranes was investigated by Jimenez et al. [32] who reported that the addition of PVP increases its molecular weight cut off (MWCO) and permeation flux of the membranes. Also, the influences of the MW of PEG on the formation of porous membranes have been studied by Kim and Lee [33], who discovered that small MWs of PEG such as PEG 200 and PEG 400 act as pore reducing agents for the polymeric membranes.

In the present research, we studied the effects of polyethylene glycol (PEG), propionic acid (PA) as a non-solvent additive, Tween-20 (polyoxyethylene sorbitan monooleate), PEG MW and polyvinyl pyrrolidone (PVP) as a pore former hydrophilic additive on morphology and performance of the synthesized hollow fiber membranes from PES/NMP&DMSO/water system in coagulation bath to obtain a membrane with the optimum performance. Permeation fluxes and total organic carbon (TOC) rejection coefficients of oily wastewater were measured for all the synthesized hollow fiber membranes. The hollow fiber membranes were prepared following the Taguchi experimental design for the minimum number of experiments. Permeation flux and TOC rejection experiments were conducted by using Taguchi experimental design. Performance of the synthesized hollow fiber membranes was optimized in such a way as to achieve high permeation flux along with reasonable TOC rejection. Additionally, Hermia's models were investigated for prediction of permeation flux decline and fouling, and then predicted results were compared with experimental data.

MATERIALS AND METHODS

1. Materials

In this work, PES (Ultrason E6020P with M_W=50,000 g/mol) supplied by BASF was used as polymer for fabrication of the spinning dope (polymer solution). These polymer flakes absorb moisture very rapidly. Thus, the flakes were dried for more than 24 h at 50 °C prior to the process. 1-methyl-2-pyrrolidone (NMP) and dimethyl sulfoxide (DMSO) with analytical purity of 99.5% (purchased from Merck) and deionized water were used as the solvent and the non-solvent agents, respectively. Polyvinyl pyrrolidone (PVP) with an average MW of 25,000 g/mol (Merck) was used as the hydrophilic polymeric additive. Polyethylene glycol (reagent grade, MW 200, 400, 1,500 and 6,000 Da) supplied by Merck was used as pore forming polymeric additive in the spinning dopes and propionic acid (PA) was also used as non-solvent additive purchased from Merck. Tween-20 (Polyoxyethylene sorbitan monolaurate, HLB= 16.7) as a surfactant additive purchased from Merck was used as a nonionic surfactant additive in the spinning dope.

2. Preparation of PES Spinning Dopes

Pre-dried (24 h oven dried at 50 °C) PES flakes were weighed and poured into pre-weighed NMP/DMSO solvent. The mixture was stirred to ensure thorough wetting of the polymer flakes, prior to the addition of appropriate amounts of non-solvent additive. To homogeneous solutions of PES/additive in NMP/DMSO, additive was added and mixed by stirring for 8 h at environment tempera-

ture. The stirring was performed at 500 rpm. The dope was kept in a graduated glass beaker (400 mL) and air bubbles formed in the dope were removed using water aspirator for several hours. The fully dissolved dope was transferred to a stainless steel reservoir and left in the reservoir for 24 h at room temperature for degassing prior to the spinning process.

3. Hollow Fiber Preparation

The dry-jet wet spinning technique was employed for preparation of the hollow fiber membranes. A spinneret with 0.6 mm inner diameter and 0.9 mm outer diameter was used. The details of the spinning parameters are listed in Table 1. During the experiments, all the spinning conditions were carefully controlled and were kept constant.

PES hollow fiber membranes were prepared by a dry-jet wet spin-

Table 1. Spinning conditions of PES and PES/PAN blended hollow fiber membranes

Parameter	Operating conditions
Bore fluid	Deionized water
External coagulant bath	Deionized water
Washing bath	Tap water
Bore fluid and external coagulation bath temperature	35 °C
Washing bath temperature	60 °C
Air gap distance	2.5 cm
Take-up speed	10 rpm
Dope extrusion rate	4.5 mL/min
Bore fluid flow rate	1.6 mL/min

(a)

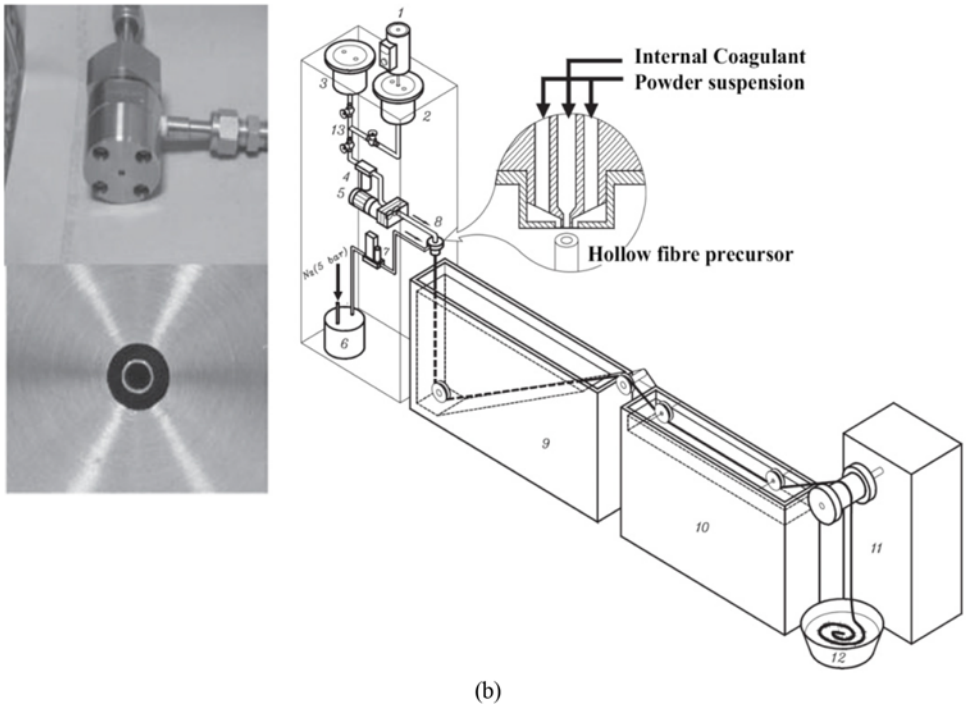

(b)

Fig. 1. Experimental set-up (a) and pilot diagram (b) for hollow fiber membranes spinning.

1. Mechanical stirrer
2. Mixing tank
3. Solution tank
4. Filter
5. Gear pump
6. Internal coagulant tank
7. Mass flow controller
8. Spinnerette
9. Coagulation bath
10. Washing bath
11. Moter guide
12. Storage tank
13. Valve

ning process as presented in Fig. 1. Fig. 1(a) and 1(b) are the experimental set-up and pilot diagram, respectively. To prepared polymer solution (dope) the powdered polymer (PES) was dissolved into a mixture of DMSO and NMP solvents. The spinning dope was synthesized from PES, additives and NMP/DMSO was used as solvent. The polymer solution was filtered over a 15 mm metal filter prior to use. The bore liquid was deionized water. Dry-jet wet spinning, as mentioned earlier, is a modification of wet spinning, where the spinneret is kept just outside the surface of coagulation bath. The spinning dope is filtered to remove any solid impurities such as gel particles (shown in Fig. 1(b)) and deaerated to remove trapped air, gasses or vapor. In dry-jet wet spinning, the polymer dope solution is metered using a gear pump and pushed through a single-hole spinneret into coagulation bath tank. The hollow fiber membrane is extruded into air environment and then is submerged inside the first coagulation bath tank. Usually, dry-jet wet spinning includes the first coagulation bath, second coagulation bath, third coagulation bath, water washing baths, drier, precision cross winder and so on, depending on the kind of process. The first coagulation bath is deep to allow vertical and coagulation of extruded fiber before it touches a guide roller (see Fig. 1(b)). The range of gap between the spinneret and the first coagulation bath surface (air gap) is about 1 to 10 cm. In this case, the extruded hollow fiber solidifies through partial crystallization, as the solvent is removed with spinning distance from the spinneret. The solidified is collected on a hollow fiber guiding wheel (bobbin) to washing baths containing non-solvent to remove traces of the solvent present inside the hollow fiber membranes.

4. Membrane Characterizations

4-1. Scanning Electron Microscopy (SEM)

The dried hollow fiber membranes were cut under liquid nitrogen and mounted on brass plates. The hollow fiber membranes were then sputter-coated with a thin film of gold. Cross-sectional images of the hollow fiber membranes were obtained using a CamScan SEM model MV2300 microscope.

4-2. Water Content and Porosity Measurement

Porous hollow fiber membranes were characterized by determination of porosity. Water content and membrane porosity play a main role in explaining their performance. To evaluate porosity of the hollow fiber membranes, they were initially impregnated with deionized water then weighed after wiping superficial water with filter papers. After that the wet hollow fiber membranes were placed in an air-circulating oven at 50 °C for 24 h to be completely dried, and finally the dry hollow fiber membranes were weighed.

The hollow fiber membrane porosity and water content was calculated using the following equations [34,35]:

$$P(\%) = \frac{W_0 - W_1}{A \cdot b} \times 100 \quad (1)$$

$$\text{Water Content } (\%) = \frac{W_0 - W_1}{W_0} \times 100 \quad (2)$$

where P is the hollow fiber membrane porosity; W_0 and W_1 are the weights of wet and dry hollow fiber membranes (gr), respectively; A is the effective area of the hollow fiber membrane (cm^2) and b is the hollow fiber membrane thickness (mm). To minimize the experimental errors, the hollow fiber membrane porosity of each sample was measured three times and the results were reported in average.

4-3. Permeation Flux and Fouling Resistance Measurement

Permeate flux (wastewater permeation fluxes) studies were performed in a batch mode. A hollow fiber membrane module made

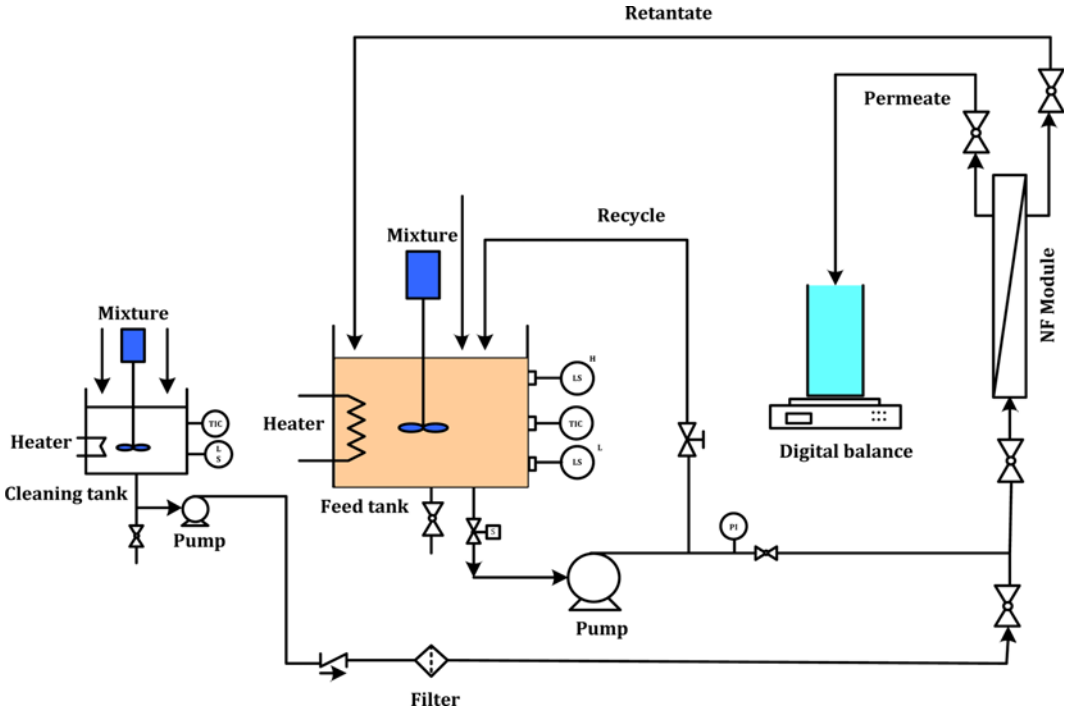

Fig. 2. Schematic diagram of laboratory scale cross flow ultrafiltration system.

from stainless steel was used in all the experiments. Each module was made with 10 hollow fiber membranes with 12 cm effective length. Membrane samples were approximately 12 cm in length, 0.8-1.1 mm in diameter and 100-150 μm in thickness. Effective area of the hollow fiber membrane in the module was 35.8 cm^2. A schematic of the setup is shown in Fig. 2. The permeation flux (J) through the membrane can be explained by the following equation [36]:

$$J = \frac{m}{A\Delta t} \quad (3)$$

where m is the collected permeate mass, A is the effective area of the hollow fiber membrane and Δt is the filtration time.

Fouling can be quantified by the resistance appearing during the filtration [37,38]. The fouling resistance is given by the following equation [37]:

$$\text{Fouling resistance} = [(PF_{wi} - PF_{ww})/PF_{wi}] \times 100 \quad (4)$$

where PF_{wi} and PF_{ww} are initial permeation flux of virgin hollow fiber membranes and final permeation flux of the fouled membrane (after filtration), respectively.

5. Experimental Procedure

The detail of the experimental setup used in this work is illustrated in Fig. 2. In the experimental trials, the cross-flow membrane system was selected. The unit included the hollow fiber membrane placed in a stainless steel module, feed and permeate tanks, feed sanitary centrifugal pump, recycle and permeate flow meters, and a heat exchanger. The considered operating conditions to conduct the membrane experiments are summarized in Table 2. The detailed experimental setup has been explained elsewhere [2,3]. The permeate flux was collected in an Erlenmeyer flask 3.0 L and measured by a digital balance. During the experiments, trans-membrane pressure (TMP), cross-flow velocity (CFV), feed temperature, pH and filtration time were carefully controlled and were kept constant.

6. Process Feed Characterizations

Oily wastewater from Tehran Oil Refining Company wastewater treatment plant was employed as feed. The characteristics of oily wastewater are key parameters for how to treat it. Oily industrial wastewater is a two-phase dispersive system in which the continuous phase is water and the dispersed phase is oil and grease content, lubricants, cutting liquids, total suspended solid (TSS), heavy hydrocarbons, and light hydrocarbons and chemical substances such as detergents, salts and caustic soda. The content of impurities depends on the kind of the process generating the effluent. For any experiments, the feed was provided daily. Organic matter is the major pollutant in industrial wastewater. Traditionally, organic matter has been measured as total organic carbon (TOC) and chemical oxygen demand (COD). Significant parameters of the samples such as chemical oxygen demand (COD), total organic carbon (TOC), turbidity, total suspended solids (TSS), and oil and grease content (OGC) were measured. For all experiments the oily industrial wastewater was sampled from the API separator unit from the Tehran Oil Refining Company (Tehran, Iran). The characteristics of the oily wastewater are shown in Table 3. Average COD, TOC, turbidity, TSS, OGC of the industrial oily wastewater was 124 mg/L, 81 mg/L, 53 NTU, 60 mg/L and 78 mg/L, respectively. Mean particle size of oil droplets in this work was set at 1.10 μm. To make sure, all parameters were measured three times and the average values were considered as presented in all tables. Standard deviations were at most 7.8%.

7. Analytical Methods

Samples prepared from the feed and the permeate for measurements of total suspended solids (TSS), chemical oxygen demand (COD), oil and grease content, turbidity and total organic carbon (TOC) were taken as necessary. The measurements were analyzed by the procedure outlined in the standard methods [39]. COD was determined by dichromate closed refluxed colorimetric method using a spectrophotometer (HACH DR/2010). Turbidity analysis was performed with a turbidimeter (Hach Model 2100A Turbidimeter, United States). TOC was obtained by TOC Analyzer (Dohrmann-Model DC-190 TOC Analyzer, Texas, United States). OGC values were analyzed by FTIR spectrometer (TOG/TPH Analyzer Infracal,

Table 2. Operating conditions of UF experiments

Parameter	Operating conditions
Feed flow rate	1 m/s
Feed liquid	Deionized water and industrial oily wastewater
Feed temperature	30 °C
Trans-membrane pressure (TMP)	3 bar

Table 3. Characteristics of the wastewater and the treated wastewater (synthesized membranes)

Parameter	Unit	Feed	Synthesized membranes				
			M2	M6	M9	M13	M15
TOC[a]	mg/L	81	4.5 (94.4%)	14.0 (82.7%)	27.1 (66.6%)	29.2 (64.1%)	6.0 (92.6%)
TSS[b]	mg/L	60	Trace (100%)	4.5 (92.5%)	6.9 (88.5%)	8.0 (86.7%)	1.1 (98.2%)
COD[c]	mg/L	124	2.1 (98.3%)	12.3 (90.1%)	21.7 (82.5%)	27.3 (78.0%)	5.9 (95.2%)
OGC[d]	mg/L	78	0.5 (99.4%)	1.9 (97.6%)	3.9 (95.0%)	4.1 (94.7%)	1.2 (98.5%)
Turbidity	NTU	53	0.4 (99.2%)	1.1 (97.9%)	3.5 (93.4%)	3.9 (92.6%)	0.9 (98.3%)

[a]Total organic carbon
[b]Total suspended solids
[c]Chemical oxygen demand
[d]Oil and grease content

Wilks Enterprise, United States). TSS values were estimated by the procedure outlined in the standard methods (ASTM 2540D) using Whatman 2.5 cm GF/C-Class Microfiber. Also, the particle size distribution was measured with Malvern equipment (LLS, MAL1008078, Malvern Instruments Ltd., United Kingdom).

8. Experimental Design

The number of experiments increases considerably with increase of the controllable factors. In this condition, the Taguchi method can be applied, which uses a special design of orthogonal arrays (OA) to study the entire factors with a small number of experiments [3]. The combination of different operating conditions was achieved by using the Taguchi experimental design method. An overview of the process performed by Taguchi approach to factor design is shown briefly and schematically in Fig. 3. The levels for each control factor should be chosen at this point. The number of levels for each controllable factor defines the experimental region.

Based on experience and the literature [18,29,31,34,35], the controllable factors (membrane preparation variables) having signifi-

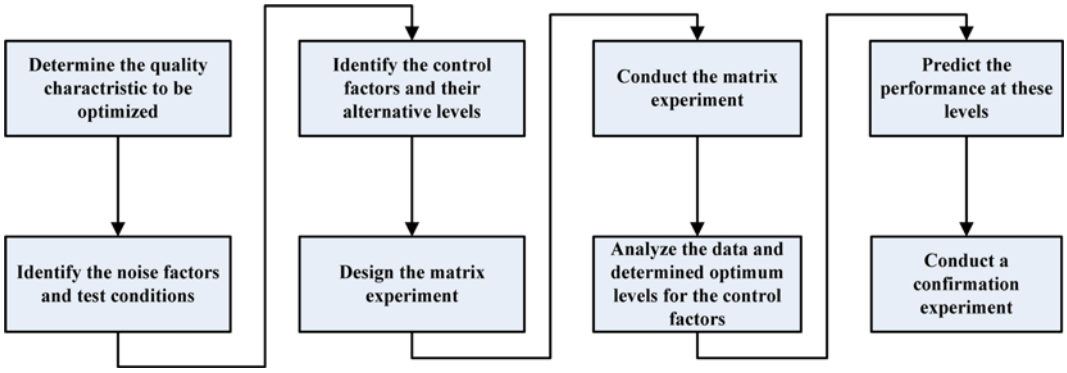

Fig. 3. Flowchart of Taguchi method.

Table 4. Hollow fiber membrane preparation variables and their levels

Controllable factors	Level			
	1	2	3	4
PEG: polyethylene glycol concentrations (wt%)	0	2.5	5.0	7.5
PA: propionic acid concentrations (wt%)	0	5	10	15
Tween 20: polyoxyethylene sorbitan monooleate (wt%)	0	1	2	4
PEG MW: PEG molecular weight (Da)	200	400	1500	6000
PVP: polyvinyl pyrrolidone concentrations (wt%)	0	3	6	9

Table 5. Experiment condition: Taguchi L_{16} design of experiments

Synthesized membrane	Polymer	Solvent		Preparation variables (polymer additives)				
	PES (wt%)	DMSO (wt%)	NMP (wt%)	PEG (wt%)	PA (wt%)	Tween 20 (wt%)	PEG MW (Da)	PVP (wt%)
M1	14	43.0	43.0	0	0	0	200	0
M2	14	38.5	38.5	0	5	1	400	3
M3	14	34.0	34.0	0	10	2	1500	6
M4	14	29.0	29.0	0	15	4	6000	9
M5	14	36.75	36.75	2.5	0	1	1500	9
M6	14	36.25	36.25	2.5	5	0	6000	6
M7	14	33.25	33.25	2.5	10	4	200	3
M8	14	33.25	33.25	2.5	15	2	400	0
M9	14	38.0	38.0	5.0	0	2	6000	3
M10	14	36.0	36.0	5.0	5	4	1500	0
M11	14	31.0	31.0	5.0	10	0	400	9
M12	14	29.5	29.5	5.0	15	1	200	6
M13	14	34.25	34.25	7.5	0	4	400	6
M14	14	31.25	31.25	7.5	5	2	200	9
M15	14	33.75	33.75	7.5	10	1	6000	0
M16	14	30.25	30.25	7.5	15	0	1500	3

cant impact on morphology and performance of synthesized membranes were selected. The detailed methodology for analysis of experimental data is described by many researchers [3,37].

The matrix experiment was designed by selecting an appropriate OA (L_{16}) and performing experiments. The PES hollow fiber membranes were synthesized based on an L_{16} OA and permeation flux and TOC rejection through them was measured. The controllable factors (hollow fiber membrane preparation variables) and their levels are presented in Table 4. The OA explained by approach L_{16} (4^5), which denotes five controllable factors (membrane preparation variables) each with four levels, was chosen and each experiment was repeated twice under the same conditions at different times to observe the effects of noise sources in the synthesized hollow fiber membranes. The interaction effects of five controllable factors (membrane preparation variables) and their levels are presented in Table 5. Based on L_{16} orthogonal array of Taguchi experimental design 32 membranes were synthesized (with two replications) and oily waste permeation flux and TOC rejection through them were measured. The factors (hollow fiber membrane preparation variables) and their levels are presented in Table 4. In this table, the columns are orthogonal and for any pair of columns all combinations of factor levels occur. The importance and significance of the controllable factors were estimated by analysis of variance (ANOVA) which was studied. Permeation flux and TOC rejec-

Table 6. Permeation flux and TOC rejection for each run

Synthesized membrane	Permeation flux		Average flux ($L/m^2 \cdot h$)	TOC rejection		Average TOC rejection (%)
	1	2		1	2	
M1	44.39	36.91	40.65	98.08	93.46	95.77
M2	95.94	108.72	102.33	94.93	93.85	94.39
M3	166.49	175.88	171.19	91.28	95.36	93.32
M4	169.22	160.98	165.10	92.76	90.12	91.44
M5	230.42	219.48	224.95	75.00	76.06	75.53
M6	202.49	198.53	200.51	84.72	80.64	82.68
M7	210.17	219.43	214.80	95.00	93.94	94.47
M8	141.18	134.20	137.69	99.54	97.98	98.76
M9	309.62	316.58	313.10	65.51	67.74	66.63
M10	316.74	309.20	312.97	89.33	87.84	88.58
M11	196.72	183.38	190.05	96.32	91.34	93.83
M12	166.13	157.51	161.82	99.67	98.67	99.17
M13	362.17	377.40	369.79	61.15	66.93	64.04
M14	295.46	300.15	297.81	77.00	74.73	75.87
M15	253.40	240.97	247.19	93.37	91.82	92.59
M16	160.20	165.86	163.03	92.06	94.97	93.52

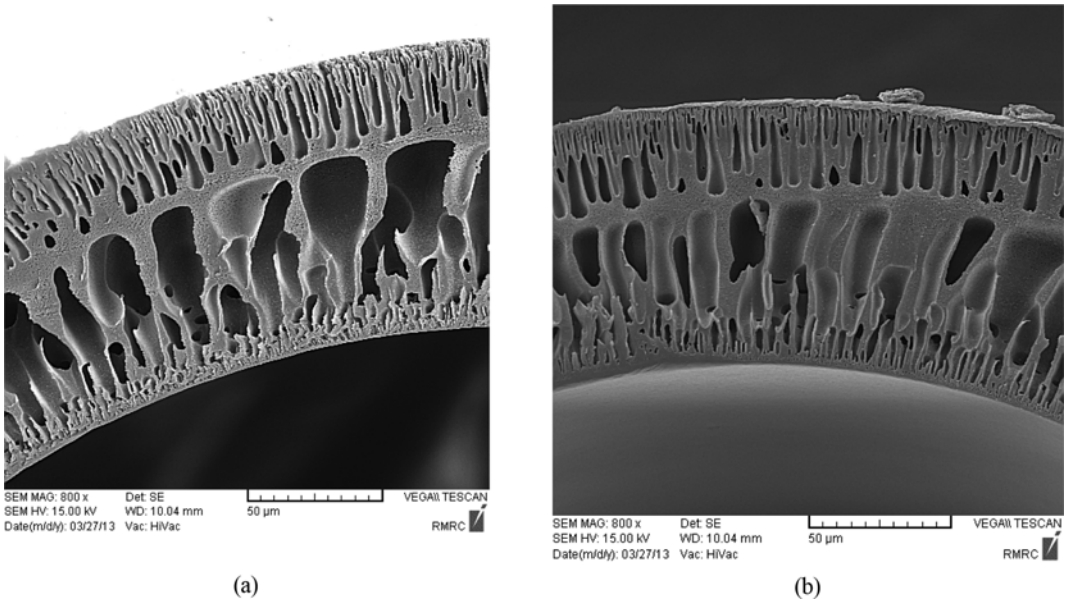

Fig. 4. SEM cross-sectional image of the synthesized PES hollow fiber membranes with different concentration of PA (wt%): (a) 0.0; (b) 10.0.

tion for each run are shown in Table 6. As can be observed, entry No. 13 (M13) and No. 13 (M8) tops all the other fourteen entries regarding permeation flux and TOC rejection, respectively.

RESULTS AND DISCUSSION

1. Effects of Non-solvent Additives Concentration on Morphology and Performance of the Hollow Fiber Membranes

1-1. Effect of PA Additive on Morphology, Water Content, Permeation Flux, and TOC Rejection of PES Hollow Fiber Membranes

The SEM images of the cross-sections of synthesized hollow fiber membranes with different concentrations of propionic acid (PA) additive in the spinning dope are shown in Fig. 4. As observed, the skin layer structures are remarkably different depending on the PA additive in the spinning dope. As observed from the SEM cross-sections images, all the synthesized hollow fiber membranes have asymmetric structure consisting of a dense top layer and a porous sub-layer with finger-like pores as well as a macrovoid structure. According to Figs. 4(a) and 4(b), the synthesized hollow fiber membranes without additive in the spinning dope have more macrovoids in cross-sections structures. From the images, the addition of PA decreases the number of microvoids. As observed in the cross-section image of the synthesized hollow fiber membranes, addition of PA to the spinning dope suppresses macrovoid growth and causes the membrane to find an asymmetric structure with finger-like pores with spongy structure of the synthesized membranes.

The PA concentration as a non-solvent additive in the spinning dope of PES was adjusted from 0.0 to 15.0 wt%. A water content measurement of the hollow fiber membrane is presented in Fig. 5. The addition of PA as a non-solvent additive to the spinning dope decreases the water content measurement of the hollow fiber membranes. Increasing PA content in the spinning dope may favor the formation of finger-like pores with spongy structure in the bottom layer of the synthesized hollow fiber membranes and suppress the macrovoid formation. According to Fig. 5, water content measurement of the hollow fiber membranes decreases from 87.5 to 63.1% when PA concentration as a non-solvent additive increases from 0.0 to 15.0 wt% in the spinning dope. This confirms that the PES hollow fibers synthesized hollow fiber membranes using more PA in the spinning dope are less hydrophilic.

Fig. 6 illustrates the effect of PA concentration on oily wastewater permeation flux and TOC rejection of the synthesized hollow

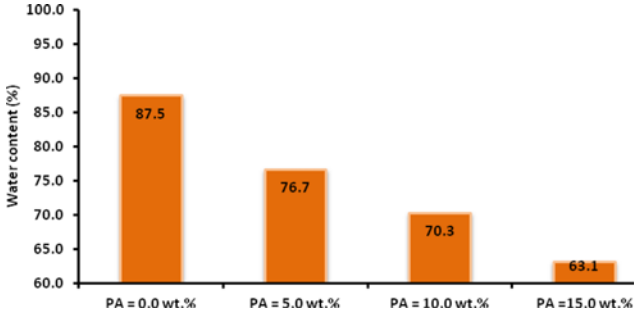

Fig. 5. Effect of PA concentration on water content (%) of the PES hollow fiber membranes.

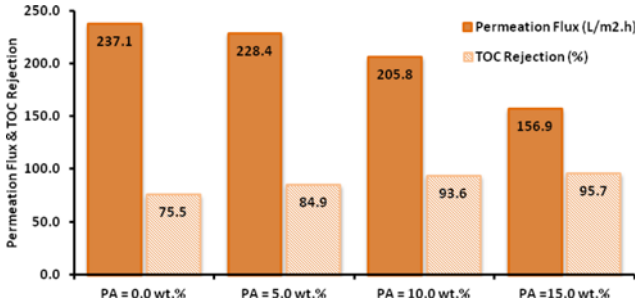

Fig. 6. Effect of PA concentration on permeation flux and TOC rejection of the PES hollow fiber membranes.

fiber membranes at a transmembrane pressure (TMP) of 3 bar, feed temperature of 30 °C and cross flow velocity (CFV) of 1 m/s. For porous hollow fiber membranes, pore size diameter and pore size distribution on the membrane morphology are the dominating parameters in permeation flux variation. Membrane structure has an important influence on improving TOC rejection and permeation flux. Mohammadi et al. observed that if the membrane pores are larger than the size of the solute particles/oil droplets, these particles/oil droplets may enter the membrane pores causing irreversible fouling [37]. When the membrane pores are smaller than the size of the particles/oil droplets present in the feed solution, these particles/oil droplets accumulate over the membrane surface causing pore sealing and/or the formation of a cake/gel layer. Overall, even tiny little changes in surface porosity can lead to significant changes in permeation flux [40]. Permeation flux through the membranes decreased by addition of PA concentration as a non-solvent additive to the spinning dope and TOC rejection increased (as can be observed in Fig. 6 for oily wastewater permeation flux and TOC rejection). When the hollow fiber membranes were synthesized without non-solvent additive in the spinning dope, permeation flux and TOC rejection through the hollow fiber membrane was 237.1 L/(m^2·h) and 75.5%, respectively. Permeation flux decreased by the addition of PA additive to the spinning dope and reached a minimum value of 156.9 L/(m^2·h) with addition of 15 wt% of PA additive to the spinning dope. Also, when 15 wt% of PA additive was added to the spinning dope, TOC rejection increased to 95.7%. This confirms smaller pore size diameter of the synthesized hollow fiber membrane using more PA additive in the spinning dope.

1-2. Effect of PVP Additive on Morphology, Water Content, Permeation Flux and TOC Rejection of PES Hollow Fiber Membranes

The cross-section SEM images of synthesized hollow fiber membranes with 0.0 and 9.0 wt% PVP in the spinning dope are presented in Fig. 7. The SEM images indicate that addition of amount of PVP in the dope solution can incite macrovoid formation. The high porosity of sub-layer of synthesized hollow fiber membranes from different concentration of PVP as additive in the dope solution, at 9.0 wt% of PVP, can be responsible for high performance of hollow fiber membranes. According to these images, higher PVP concentrations caused greater formation of macrovoids and more porous structures. Increasing PVP concentration from 0.0 to 9.0 wt% in the spinning dope causes the sub-layer of the hollow fiber membranes to have more big macrovoids (approximate value 30 μm), and the shape of macrovoids in the hollow fiber membranes

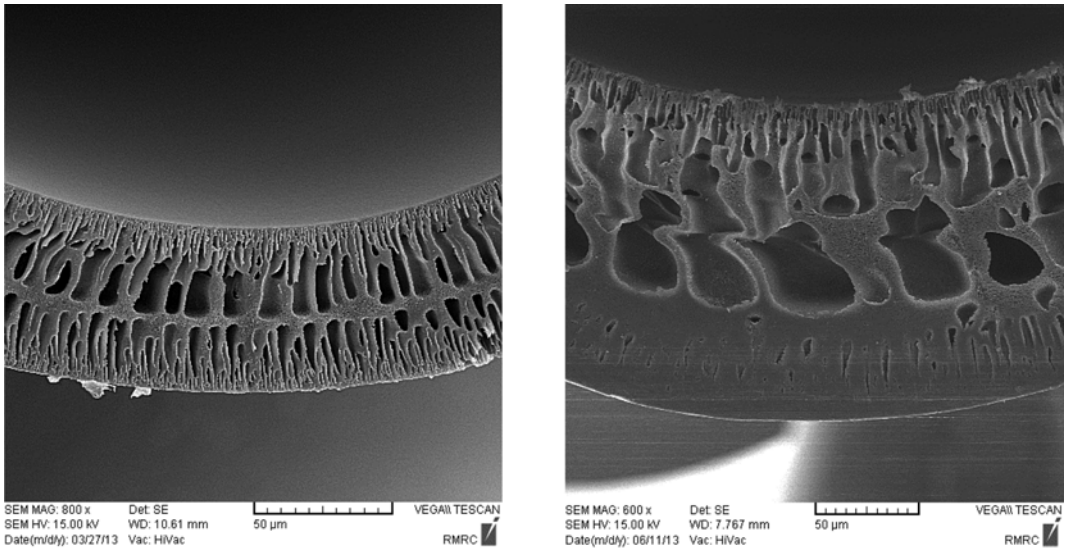

Fig. 7. SEM cross-sectional image of the synthesized PES hollow fiber membranes with different concentration of PVP (wt%): (a) 0.0; (b) 9.

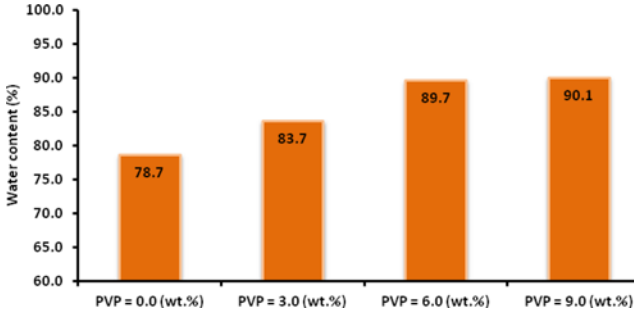

Fig. 8. Effect of PVP concentration on water content (%) of the PES hollow fiber membranes.

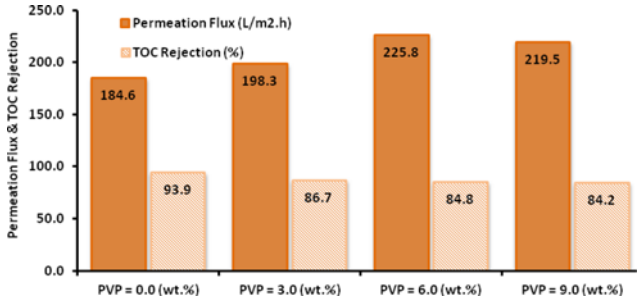

Fig. 9. Effect of PVP concentration on permeation flux and TOC rejection of the PES hollow fiber membranes.

sub-layer change. In generally, the addition of PVP additive, to the spinning dope has a dual effect on the membrane morphology (increases thermodynamic instability and increases viscosity) [29]. The final structure depends on superiority of delayed demixing. In this work (see Fig. 7 (SEM)) increasing PVP concentration causes formation of greater macrovoids and more porous morphologies.

Hydrophilicity is one of the important properties of hollow fiber membrane that greatly affects their permeation flux, rejection and fouling resistance ability. Water content was measured to evaluate the effects of PVP content on hydrophilicity and surface properties of the asymmetric hollow fiber membranes. Fig. 8 represents the effect of PVP concentration on water content of the PES hollow fiber membranes. It can be observed that the lowest water content for the hollow fiber membrane was obtained with no PVP additive in the spinning dope. This confirms the lowest hydrophilicity of this hollow fiber membrane. Increasing the PVP content in the spinning dope increases the water content of the PES membrane [41,42]. This means the hydrophilicity of the hollow fiber membranes increases by increasing the PVP content.

Fig. 9 shows the effect of PVP content on permeation flux and TOC rejection of the synthesized hollow fiber membranes. This Figure demonstrates the variation of permeation flux against PVP content. Permeation flux increases at low PVP content and decreases at high PVP content. So, increasing PVP content has two different effects on permeation flux. According to the experimental data indicated in Fig. 9, at lower PVP content, permeation flux increases by increasing PVP content, but at higher PVP content, permeation flux decreases slightly by increasing PVP content. As a result, the product of permeation flux varies with PVP content and it has two negative and positive slopes and a maximum value. For porous asymmetric membranes (UF and MF), pore diameter and pore size distribution in the collapsed PES nodules on the hollow fiber membrane structure is the dominating parameter in permeation flux. A little change in membrane morphology such as surface porosity or waster content can lead to significant changes in permeation flux [42]. The permeation flux increases and reaches a maximum with the addition of 6.0 wt% PVP content and then decreases with the further addition of PVP content in the spinning dope. Optimum values of the oily wastewater permeation flux were observed for the synthesized hollow fiber membrane with 6.0 wt% of PVP content in the spinning dope. According to Fig. 9, TOC rejection decreases as PVP content increases. The results show that oily wastewater permeation flux and the TOC rejection for the synthesized

hollow fiber membrane from the spinning dope without PVP content are 184.6 L/(m^2·h) and 93.9%, respectively. While 6.0 wt% PVP content is added to the spinning dope, the oily wastewater permeation flux increases to 225.8 L/(m^2·h) and the TOC rejection decreases to 84.8%. According to the results, the oily wastewater permeation flux decreases and the TOC rejection slightly increases at higher concentration of PVP content in the spinning dope (9.0 wt%).

1-3. Effect of Tween-20 Additive on Morphology, Water Content, Permeation Flux and TOC Rejection of PES Hollow Fiber Membranes

The addition of Tween-20 additive in the spinning dope may have two main effects on the membrane formation processes: (i) a decline of the solvent evaporation rate, and (ii) a diminished interaction between polymer chain due to formation of polymer-surfactant complex [43]. The hollow fiber membrane performance is a function of membrane morphology properties [44]. For a hydrophilic coagulant, hydrophilic surfactants are able to improve the macrovoid formation and hydrophilicity of the hollow fiber membranes. In this research, the effects of Tween-20 additive as a nonionic surfactant on membrane morphology, permeation flux and TOC rejection of the PES hollow fiber membranes are studied. The cross-sectional SEM micrographs of synthesized membranes with 1.0 and 4.0 wt% Tween-20 in the spinning dope are represented in Fig. 10. Comparison between images in Fig. 10 depicts that addition of Tween-20 in the spinning dope leads to membranes containing more porous sub-layer with smaller finger like pores. In addition, the shapes of finger-like pores were turned from tilted to straight. This phenomenon could be described by the miscibility between the used surfactant (Tween-20) and the non-solvent. The changes in the hollow fiber membrane morphology can be attributed to, and described by, the interactions between components in the spinning dope and phase inversion kinetics. When the concentration of Tween-20 in the spinning dope is increased, the interaction between Tween-20 and NMP/DMSO is improved. The effect of addition of Tween-20 as surfactants in the dope solution for formation of macrovoids in polymer membranes was investigated by Wang et al. [45]. Strathmann et al. studied that highly porous membranes can be synthesized when the non-solvent enters the nascent membrane faster than the solvent escapes, although dense membranes can be synthesized when the solvent escapes faster than the non-solvent enters [46]. Also, the effect of addition of Tween-20 on the morphology and microfiltration (MF) performance of asymmetric PES membranes is reported by Amirilargani et al. [47]. The miscibility between the added Tween-20 and the non-solvent (water) plays an important role in the formation process of macrovoids [45]. The macrovoids and finger-like pores can be induced by addition of resulting surfactants (Tween-20), depending on their miscibility with the non-solvent. A formation mechanism of macrovoids was suggested by Smolders et al. [48]. Rahman et al. [49] also discovered that surfactant additive in the dope solution plays an important role in macrovoid formation.

The SEM images of the cross-sections of the synthesized membranes with high concentration (4.0 wt%) of Tween-20 as a surfactant additive (shown in Fig. 10(b)) demonstrate that addition of large amount of Tween-20 to the spinning dope can be incite macrovoids formation.

Hydrophilic additives are able to improve the pore size, pore size distribution and hydrophilicity of the hollow fiber membranes. Membrane experiments were carried out to study membrane performance (flux and rejection properties). The results are shown in Fig. 11. It can be observed that the permeation flux of PES hollow fiber membranes increases by increasing Tween-20 content in the spinning dope. For example, the permeation flux value is the highest for 4.0 wt% of Tween-20 content and the lowest for without of Tween-20 content in the spinning dope. Permeation flux of synthesized hollow fiber membrane without Tween-20 in the spin-

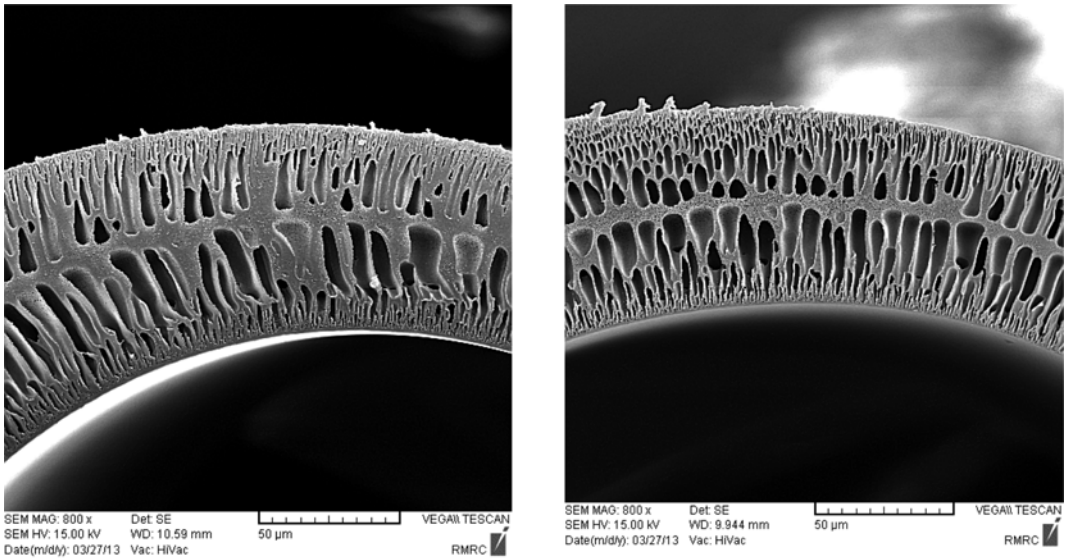

Fig. 10. SEM cross-sectional image of the synthesized PES hollow fiber membranes with different concentration of Tween-20 (wt%): (a) 1.0; (b) 4.0.

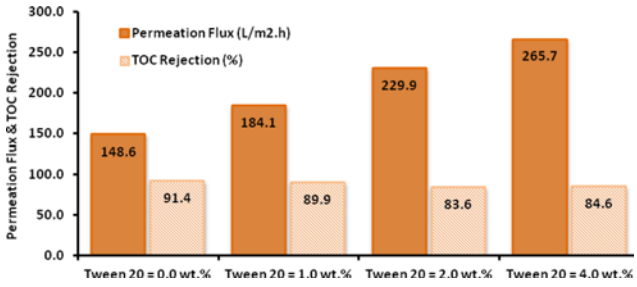

Fig. 11. Effect of Tween-20 concentration on permeation flux and TOC rejection of the PES hollow fiber membranes.

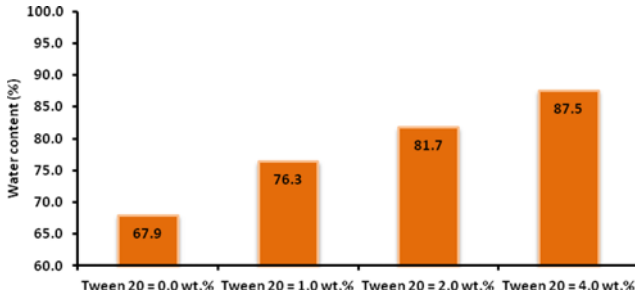

Fig. 12. Effect of Tween-20 concentration on water content (%) of the PES hollow fiber membranes.

ning dope is 148.6 L/(m^2·h) and increases to 265.7 L/(m^2·h) by addition 4 wt% of Tween-20 additive to the spinning dope. Increasing permeation flux of the synthesized PES hollow fiber membranes via addition of Tween-20 as surfactant additive to the spinning dope may be due to combined effects of porosity and hydrophilicity of the PES hollow fiber membranes.

Oily wastewater permeation flux of the PES hollow fiber membranes is presented in Fig. 11. According to these results, permeation flux increases with increasing Tween-20 content in the spinning dope. The effect of Tween-20 content on the TOC rejection through the PES hollow fiber membranes is given in Fig. 11. In general, the TOC rejection decreases by increasing Tween-20 content in the spinning dope. For example, TOC rejection decreases from 91.4 to 84.6% when the Tween-20 content increases from 0.0 to 4.0 wt%. This TOC rejection reduction can be due to the fact of macrovoid formation in the membrane morphology by increasing the Tween-20 content.

Fig. 12 shows the water content of the synthesized hollow fiber membranes according to Eq. (2). As observed, the addition of Tween-20 content to the spinning dope enhances water content of all the hollow fiber membranes. For example, water content of the hollow fiber membrane increases from 67.9 to 87.9%, when Tween-20 content in the spinning dope increases from 0.0 to 4.0 wt%. Addition of Tween-20 as a hydrophilic surfactant additive to the spinning dope may favor formation of greater pores in the support layer of the synthesized hollow fiber membranes, and as a result, the hollow fiber membranes become more porous. When the Tween-20 additive content increases, repulsive forces between the PES segments along with leachability of the additive are enhanced and this favors formation of macrovoids due to occurrence of greater number of larger pores [50].

1-4. Effect of PEG Content on Morphology, Water Content, Permeation Flux and TOC Rejection of PES Hollow Fiber Membranes

Cross-sectional SEM images of the two synthesized hollow fiber membranes at 0.0 wt% and 5.0 wt% of PEG concentrations and constant values of PES concentration, CBT and PEG MW (17.0 wt%, 30 °C and 6,000 Da, respectively) are shown in Fig. 13. Increasing PEG concentration causes formation of greater macrovoids and more porous structures. Note the influence of hydrophilic additives on the hollow fiber membrane structure. The membrane that

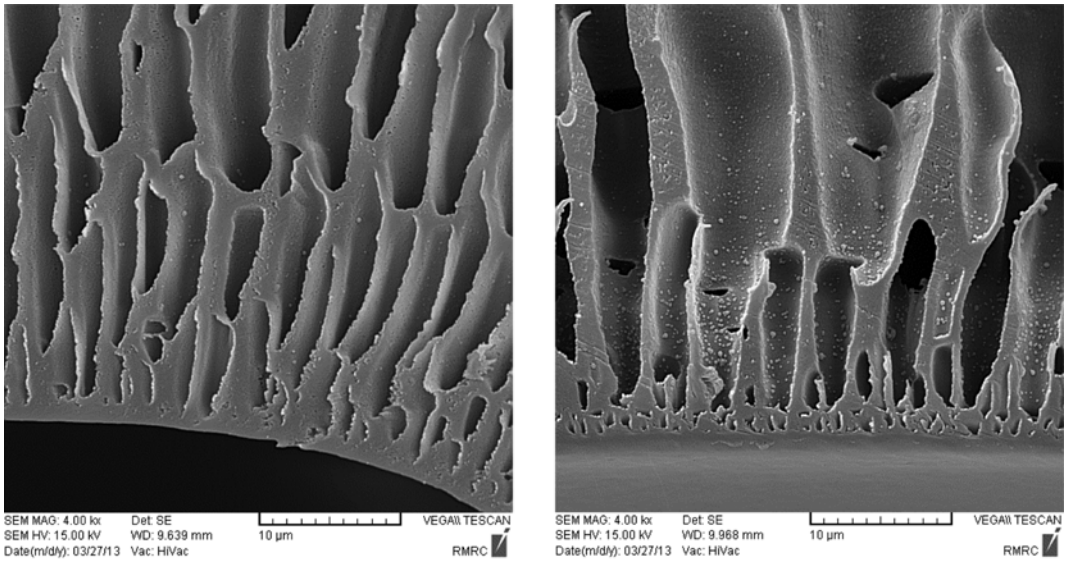

Fig. 13. SEM cross-sectional image of the synthesized PES hollow fiber membranes with different concentration of PEG (wt%): (a) 0.0; (b) 5.0.

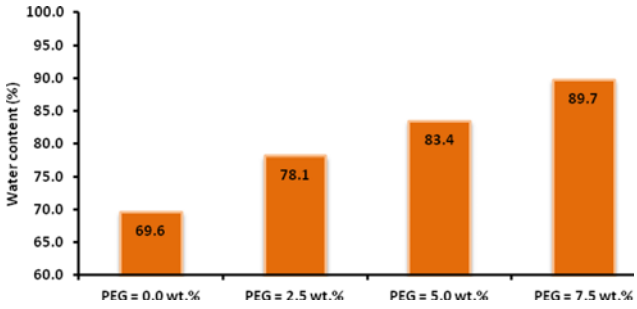

Fig. 14. Effect of PEG concentration on water content of the PES hollow fiber membranes.

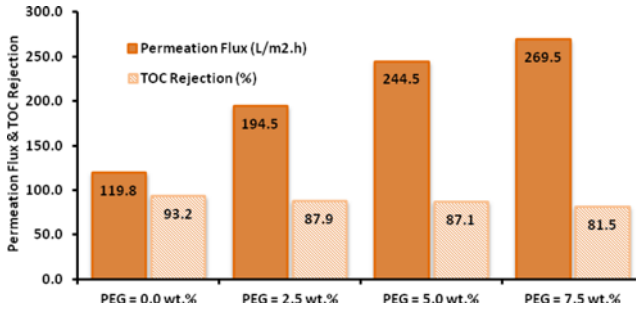

Fig. 15. Effect of PEG concentration on permeation flux and TOC rejection of the PES hollow fiber membranes.

synthesized without PEG in the spinning dope has finger-like macrovoids that end halfway, and there are some macrovoids in the bottom layer of the hollow fiber membranes. The number and size of finger-like pores in the cross-sectional of this hollow fiber membrane is more and smaller, respectively. By increasing the concentration of PEG additive in the spinning dope from 0.0 to 5.0 wt%, the membrane morphology changes from spongy structure with thin finger-like structure in the sub-layer to long and wide finger-like structure with some bigger macrovoids. Amirilargani et al. reported addition of the additives that have high miscibility with the non-solvent may be able to enhance the formation of finger like pores and macrovoids [47].

For the PES hollow fiber membranes, water content, pore size and porosity of membranes are dominating parameters affecting permeation flux and TOC rejection in wastewater treatment. Water content, which is a main factor in porous membrane characterization, is mainly controlled by porosity and permeation flux of hollow fiber membranes. Water content is calculated from Eq. (2) and reported in Fig. 14. It is observed that addition of PEG content to the spinning dope enhances average water content of all the membranes. For example, the water content of the PES hollow fiber membranes increases from 69.6 to 89.7%, when PEG content in the spinning dope increases from 0.0 to 7.5 wt%. Addition of PEG content as hydrophilic surfactant additive to spinning dope may favor formation of larger pores in the support layer of the synthesized membranes. When additive concentration increases, repulsive forces between polymer segments along with leachability of the additive enhance and this favors formation of macrovoids due to occurrence of more number of larger pores [51-53].

According to Fig. 15, increasing PEG content in the spinning dope increases permeation flux and decreases TOC rejection due to the trade-off between the permeation flux and the TOC rejection. Addition of 7.5 wt% PEG to a PEG free spinning dope increased permeation flux of the PES hollow fiber membrane from 119.8 to 269.5 L/(m^2·h), while TOC rejection decreased from 93.2% to 81.5%. It shows that PEG, as a hydrophilic additive, changes the membrane morphology in a manner that the permeation flux increases and whereas TOC rejection slightly decreases.

In the present research, the addition of PEG from 0.0 wt% to 7.5 wt% enhanced formation of macrovoids in the hollow fiber membrane structure and therefore increased permeation flux and subsequently decreased TOC rejection (see Fig. 15).

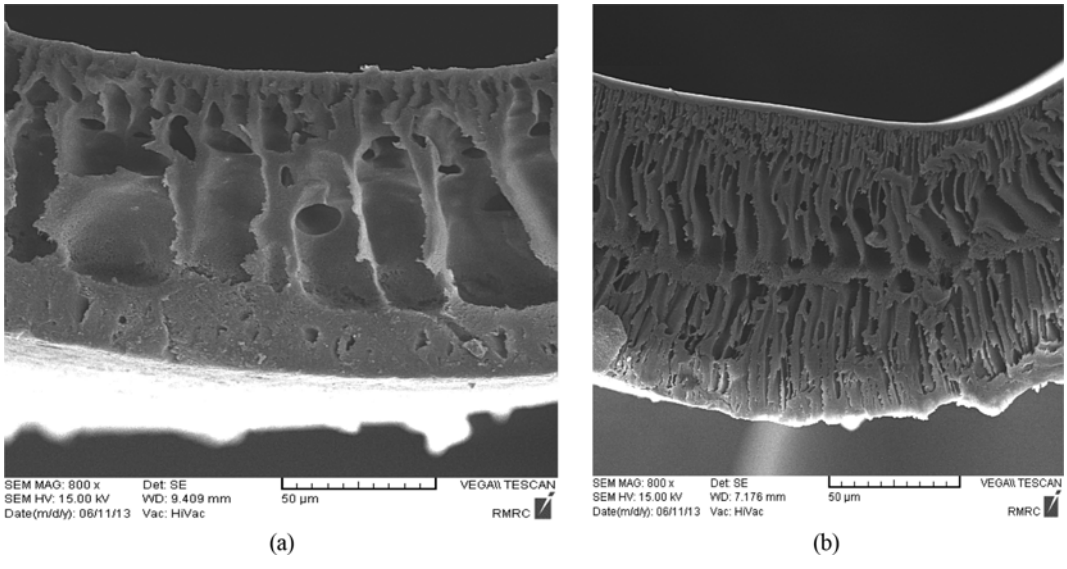

Fig. 16. SEM cross-sectional image of the synthesized PES hollow fiber membranes with different MW of PEG (wt%): (a) 200; (b) 6000.

Eventually, it could be deduced that increasing content of hydrophilic additives in the spinning dope increases porosity of the synthesized membranes. Similar results for polymeric membranes (such as cellulose acetate) using PEG as additive and solvent (such as NMP) were observed by others [54-58].

1-5. Effect of Molecular Weight of PEG on Morphology, Water Content, Permeation Flux and TOC Rejection of PES Hollow Fiber Membranes

The cross-section SEM micrographs of the synthesized hollow fiber membranes at various PEG MWs (200 and 6,000 Da) and constant PES concentration, CBT and PEG concentration (17.0 wt%, 30 °C and 5.0 wt%, respectively), are represented in Fig. 16. Amirilargani and Mohammadi [59] reported that the distance from top layer of the membranes to starting point of macrovoid formation decreases by increasing PEG MW additive. SEM observations also indicated that increasing PEG MW number and size of finger-like pores in the cross-section of this hollow fiber membrane is more and smaller, respectively. In the synthesized membranes with NMP/DMSO as solvent in the spinning dope, increasing the MW of the PEG additive from 200 to 6,000 Da, changes the size of the macrovoids gradually in structure from a tear drop shape to elongated macrovoids. The synthesized membranes with PEG 200 as additive have finger-like pores macrovoids that end halfway, and there are some macrovoids in the bottom layer of the synthesized hollow fiber membranes. The result shows that, increasing PEG MW additive causes formation of smaller macrovoids and more porous structures. It may be that the influence of hydrophilic additives on the membrane morphology and its permeability intensively depends on MW of the additives [5,30-32].

Fig. 17 shows the effect of PEG MW on permeation flux and TOC rejection of the synthesized membranes from PES/PEG/NMP&DMSO system in water coagulation bath. The addition of PEG MW to the spinning dope results in an increase in permeability and rejection of the synthesized hollow finer membranes. For example, when the membrane is synthesized with PEG MW 200 Da in the spinning dope, permeation flux of the membrane is 178.8 L/(m^2·h). Permeation flux increases by addition of PEG MW to the spinning dope and reaches to a maximum value of 231.5 L/(m^2·h) by MW of 6,000 Da of PEG to the spinning dope. Addition of PEG MW to the spinning dope increases porosity of the membrane support layer and this results in higher permeation flux. High sub-layer porosity of the synthesized membranes from different MW of PEG as additive in the spinning dope, can be responsible for high performance (higher permeation) of the membranes.

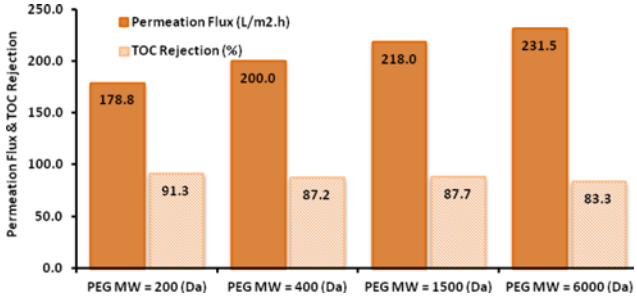

Fig. 17. Effect of PEG MW on permeation flux and TOC rejection of the PES hollow fiber membranes.

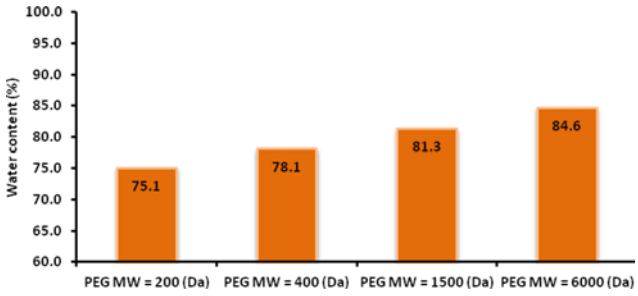

Fig. 18. Effect of PEG concentration on water content of the PES hollow fiber membranes.

Also, in general the TOC rejection decreases by increasing PEG MW in the spinning dope (see Fig. 17). For example, TOC rejection decreases from 91.3 to 83.3% when the PEG MW increases from 200 to 6,000 Da. This TOC rejection reduction can be due to macrovoid formation in the membrane structure by increasing the PEG MW.

Water content is a main factor in hollow fiber membrane characterization as it is closely related to permeation flux of polymeric and ceramic membranes. Water content of the synthesized hollow fiber membranes determined using Eq. (2) is shown in Fig. 18. The addition of PEG with higher MW to the spinning dope enhances the water content of all the hollow fiber membranes. According to Fig. 18, for the PES/DMSO&NMP/PEG hollow fiber membrane, the water content increases from 65.1% to78.8% when the MW of PEG increases from 200 to 6000 Da. This increasing trend confirms that the higher MW in the spinning dope of PEG the more pores in the hollow fiber membranes.

As illustrated in Fig. 18, the variation in water content of the PES membranes with the MW of PEG in the spinning dope was calculated using Eq. (2). The result shows that the membrane water content increases from 75.1 to 84.6% for the PES/DMSO&NMP/PEG hollow fiber membranes when MW of PEG used in the spinning dope increases from 200 to 6,000 Da. The effect of MW of PEG on the water content of the hollow fiber membranes can be considered on the basis of thermodynamics and kinetics. The addition of polymeric additives such as PEG into the spinning dope can affect the phase separation during the hollow fiber membrane formation process by thermodynamic enhancement (reducing the miscibility) and kinetic hindrance (increasing the viscosity) [34,35,49,51]. According the results of the experiments, this could influence the exchange rate between the solvent and the non-solvent during the phase separation process, which according to the theory reported by Young and Chen [60] results in porous membranes. Thus, the addition of PEG 6,000 Da to the spinning dope decreases the miscibility of the spinning dope with water and increases the porosity of the synthesized membranes.

2. Experimental Performance Evaluation of Synthesized Membranes for Treatment of an Industrial Oily Wastewater

Experimental performance of the synthesized hollow fiber membranes for industrial at the operating conditions (TMP of 3 bar, feed temperature of 30 °C, pH of 7.5 and CFV of 1 m/s) was investigated. The permeation flux versus filtration time of synthesized

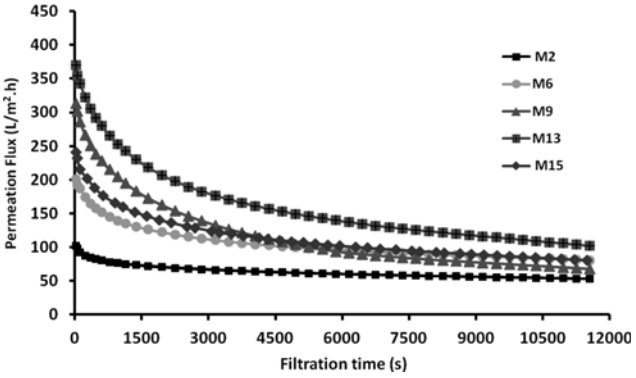

Fig. 19. Permeation flux of synthesized hollow fiber membranes for industrial oily wastewater (TMP=3 bar, CFV=1 m/s, feed temperature=30 °C).

membranes during industrial oily wastewater treatment is shown in Fig. 19. The variation of permeation flux can be divided into two stages, a sharp decay and a pseudo-steady stage. At the early period of filtration, the permeation flux reduces very quickly due to the rapid membrane blocking and particles/oil droplets deposition. The reduction rate in permeation flux becomes very slow during 1,500 s. In fact, the permeation fluxes approach to their pseudo-steady values. After 4,500 s filtration, because of formation of a secondary layer (cake/gel layer) on the membrane surface, the permeate fluxes reach to 55-144 L/(m^2·h) by 38-65% decline. From the results indicated in Table 3, the oily industrial wastewater has large content of TSS, lubricants, cutting liquids, heavy naphtha (such as tars, fuel oil, crude oils, grease and diesel oil), and light naphtha (such as kerosene, blending naphtha, jet fuel and gasoline). The oily wastewater was treated by different synthesized hollow fiber membranes. During the experiments, CFV, feed temperature, TMP and filtration time were carefully controlled and were kept constant. One of the major benefits of synthesized hollow fiber membranes is their ability to cope with high levels of oil and grease content, turbidity and TSS. Table 3 represents characteristics of the feed and the permeate (rejection) regarding oil-grease content (OGT), TSS, turbidity, TOC and COD during treatment of the industrial oily wastewater for 11600 s. The data indicate that the fouling resistance (%, calculated using Eq. (4)) for M9 was higher than that for the other membranes. According to the results of the experiments, fouling resistance for the M2, M6, M9, M13 and M15 synthesis hollow fiber was about 48.1%, 59.7%, 78.3%, 72.4% and 66.7%, respectively. The obtained results demonstrate the oil-grease content in the permeates of the M2, M6, M9, M13 and M15 synthesis hollow fiber membranes were 0.5, 1.9, 3.9, 4.1 and 1.2 mg/L, respectively. As expected, the rejection of the M2 membranes was more than that of the other synthesis hollow fiber membranes. This was due to the smaller pores and the more hydrophilic nature of the M2 membranes, which significantly rejects oil emulsion droplets (shown in Table 3). In the all experiments, the M2 membranes performed better than the other synthesis membranes (M6, M9, M13 and M15), and regarding TSS and turbidity values, the difference was more considerable. The synthesized membranes were found practically suitable to treat that oily wastewater with the rejections of OGT at the level of 94.7-99.4% resulting in permeates with OGT below 5 mg/L, and thus the process can meet the level set in the environmental regulations.

These results show the ability of synthesized hollow fiber membranes for oily wastewater treatment in oil refining manufacturing plant. Ultimately, the M13 membrane was more suitable than the other synthesized hollow fiber membranes because of its higher permeation flux (102.2 L/(m^2·h)), higher rejection (64.1.0% of TOC and 94.7% of OGC), and lower fouling resistance (72.4%) for the oily wastewater treatment of Tehran Oil Refining Company.

3. Modeling and Prediction of Permeation Flux by Hermia's Models

Many theoretical models about prediction of fouling resistance or permeation flux have been suggested recently. However, when solute particles/oil droplets size is smaller than or comparable to the membrane pores, the membrane blocking model is commonly a useful tool to explain how and when the solute particles/oil droplets penetrate into or block the pores. The experimental data was fitted to Hermia's models to investigate the mechanism of membrane fouling [61]. The cake layer formation model was studied in terms of several kinetic models [62-64]. As can be observed, if the membrane pores are smaller than the solute particles/oil droplets, these particles/oil droplets accumulate over the membrane surface, causing pore sealing and/or the formation of a gel layer. However, the occurrence of the opposite shows that the membrane pores are larger than the solute particles/oil droplets present in the oily wastewater; these particles/oil droplets cannot enter the membrane pores, resulting in reversible fouling resistance. Eventually, solute particles/oil droplets of a similar size to that of the membrane pores may result in a partial blocking of them. The filtration mechanism (pre-

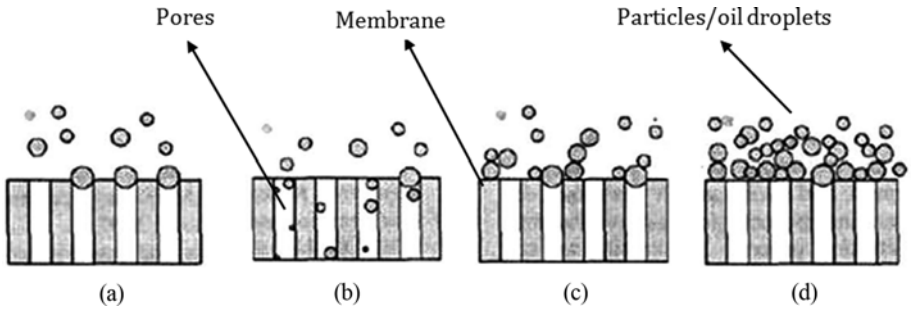

Fig. 20. Schematic representation of blocking mechanisms, complete pore blocking (a), standard blocking (b), intermediate blocking, (c) and cake layer formation (d).

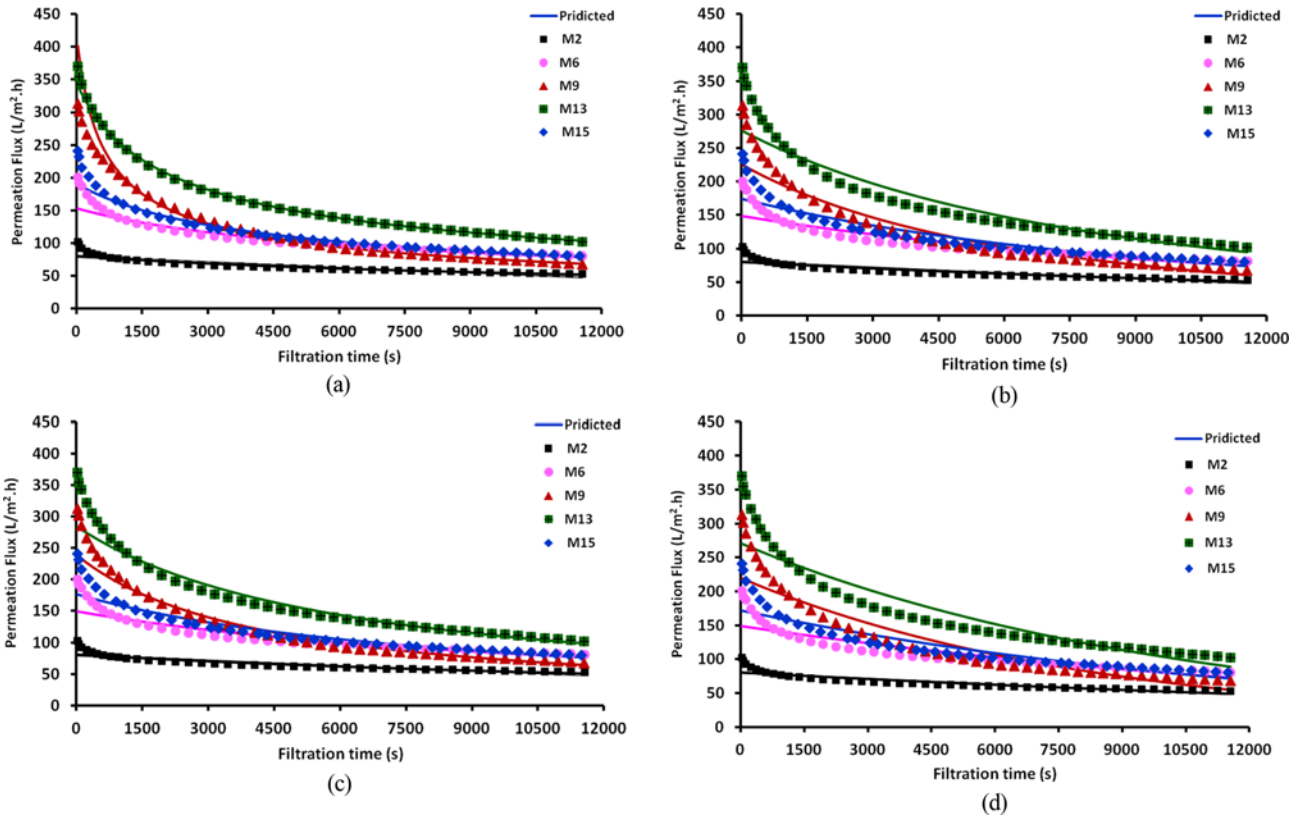

Fig. 21. Permeation flux predicted by the Hermia's models model for synthesized hollow fiber membranes: (a) Cake layer formation model; (b) standard pore blocking model; (c) intermediate pore blocking model and (d) complete pore blocking model (lines: predicted data; symbols: experimental results).

diction of fouling resistance or permeation flux) was determined to elucidate the occurrence of adsorption, i.e., membrane surface or internal pores.

In following section, Hermia's models were applied to study the fouling phenomenon occurring in the synthesized hollow fiber membranes of oily wastewater. Fitting of experimental data to these models permits one to distinguish whether permeation flux decline was controlled by pore blocking models. The different types of pore blocking mechanisms for membrane fouling are shown in Fig. 20. The pore blocking models include standard pore blocking (inside of the pores), intermediate pore blocking, complete pore blocking or cake/gel layer formation (outside of the pores). In the standard pore blocking, solute particles/oil droplets go completely inside the membrane pores, whereas if pore blocking occurs outside the membrane pores, the solute particles/oil droplets causing pore blocking may have a similar size to that of the membrane pores and they are partially introduced inside the membrane pores (intermediate pore blocking) or may be bigger than the membrane pores (complete pore blocking) [62-65].

Most models of membrane fouling resistance correlate the permeation flux with the filtration time in terms of a polynomial relationship by using pore blocking, adsorption, cake/gel formation, and bio-fouling [61-64]. The details of the model equations for flux decline prediction have been explained elsewhere [61,65]. The generated plots are in Figs. 21(a) to 21(d).

Fig. 21(a) illustrates the fitting of cake/gel layer formation model to the experimental data for the synthesis hollow fiber membranes (M2, M6, M9, M13 and M15). The model predictions of permeation flux are indicated to be in reasonable agreement with the experimental results because most of the particles/oil droplets are retained by the synthesis hollow fiber membranes. Lowest deviations between experimental and predicted permeation flux decline were observed

Table 7. R^2 values of Hermia's models for synthesized hollow fiber membranes

Synthesized membrane	Cake filtration	Standard pore blocking	Intermediate pore blocking	Complete pore blocking
M2	0.9491	0.8836	0.9088	0.8552
M6	0.9685	0.8834	0.9211	0.8500
M9	0.9979	0.9526	0.9815	0.9083
M13	0.9900	0.9487	0.9576	0.9076
M15	0.9934	0.9243	0.9572	0.8815

in the cake filtration model. According to the results listed in Table 7 and presented in Fig. 21, deviation of the experimental results from the cake/gel layer formation model prediction is less than 0.6%. The cake layer formation mechanism occurs when particles/oil droplets are larger than the membrane pore size. Therefore, they are unable to enter the hollow fiber membrane pores. Cake layer thickness, oil droplet deformation and cake compression are the main factors influencing the cake/gel layer resistance (shown in Fig. 19). The cake/gel layer thickness and oil droplet deformation may increase packing density of the cake/gel layer formed, and thus may favor a higher cake/gel resistance (fouling resistance) and a lower permeation flux.

The standard pore blocking occurs when the membrane pores are larger than the size of the particles/oil droplets present in the oily wastewater. An internal pore blocking is carried out due to the adsorption of particles/oil droplets onto the membrane pores walls. Fig. 21(b) shows that the standard blocking model cannot be accurately fitted to the experimental data for the synthesis membranes (M2, M6, M9, M13 and M15). As observed, the standard pore blocking model can only predict permeation flux decline at higher permeate flux accurately, e.g., for the M9 and M13 synthesis membranes. In fact, it can be due to that oil droplets are retained by the membrane, because most of the particles/oil droplets in the oily wastewater are larger than the membrane pores.

The intermediate pore blocking occurs when the size of particles/oil droplets is similar and larger to the size of membrane pores. Membrane pores are blocked near their entrances in the oily wastewater side. As observed, the intermediate blocking model provides reasonable agreement with the experimental results. Fig. 21(c) indicates that the fitting of the intermediate pore blocking model to the experimental permeation flux data for the synthesis membranes (M2, M6, M9, M13 and M15), especially at operating conditions that correspond to high variation of permeation flux with filtration time; the lowest for M2 (see Table 7). This could be because most particles/oil droplets are retained by the membrane, because most of the particles/oil droplets in the oily wastewater are larger than the membrane pores.

Fig. 21(d) shows the fitting of the experimental permeation flux for the synthesis hollow fiber membranes to the complete pore blocking model. The highest deviations between the experimental results and the predicted permeation flux decline values are found for the M6. The complete pore blocking typically occurs when particles/droplets are dimensionally similar to the mean pore size of the membrane. As a result, particles/oil droplets do not enter into the membrane pores and they do not arrive the permeate side. As a result, particles/droplets plug individual pores. As individual pores are plugged, the flow is diverted to other pores, which plug successively. Finally, this reduces the effective area of the membrane and increases the membrane fouling resistance. When fouling resistance occurs, the membrane loses its permeability and requires replacement, chemical cleaning or back washing. According to this condition, differences between the experimental results and the predicted data can be related to the fact that some particles/oil droplets permeate due to some higher pores of the synthesis hollow membrane.

Fig. 21 (a) to (d) demonstrates the fitting of Hermia's models to the experimental data obtained in this research. The solid lines and symbols are the model predictions and the experimental data, respectively. Table 7 shows the calculated R^2 values. When R^2 values obtained for the same model are compared at different synthesized membranes, according to the results listed in Table 7 and presented in Fig. 21, it can be deduced that the higher R^2 value corresponds to a better fit of the model. The estimated model parameters from Fig. 21 indicate that the filtration is cake dominating in synthesized hollow fiber membranes. High deviations between the experimental results and predicted permeation flux were observed for standard pore blocking and complete pore blocking, but the cake filtration model and intermediate pore blocking provided a reasonable agreement (best fit) to the experimental results than the other models, as was expected.

From the observation of Table 7 it can also be concluded that the best fit to experimental data for the experimental conditions tested corresponds to the cake layer formation model; also the intermediate pore blocking model can reasonably predict the experimental results.

The results showed that the cake layer formation model and the intermediate pore blocking models have better prediction than the standard and the complete pore blocking models. The results demonstrated that fitting of the standard pore blocking model to the experimental results is not good enough for the synthesized hollow fiber membranes. Note that the highest deviation between the experimental results and the predicted permeation flux decline were observed for the complete pore blocking model. Average error of the predicted permeation flux for the cake layer formation, intermediate, standard, and complete pore blocking models was 2.02%, 8.15%, 5.48%, and 11.95%, respectively. For all the models used in this work, the accuracy of the fitted results is high when permeation flux slightly varies with filtration time.

CONCLUSION

PES hollow fiber membranes were synthesized using dry-jet wet spinning process. Various amounts of additives were used as non-solvent additives in the spinning dopes to improve the phase-inversion rate and provide porous asymmetric hollow fiber membranes with improved structure for oily wastewater treatment. The L_{16} (4^5, five controllable factors each with four levels) OA of Taguchi experimental design was applied to conduct a minimum number of experiments. Effects of PA concentration, PEG concentration, PEG MW, Tween-20 concentration and PVP concentration on morphology of the synthesized membranes and their permeation flux as well as TOC rejection for an oily wastewater system were investigated. Measurement techniques such as membrane structure, water content, permeability, and TOC rejection were used to evaluate membrane performance.

The obtained results indicate that addition of small amounts of non-solvent additives in the spinning dopes (i.e., PEG, Tween-20 and PVP) increases formation of macrovoids and finger-like pores in the hollow fiber membranes. With this little addition of non-solvent additives to the spinning dopes, water content and permeation flux of the synthesized hollow fiber membranes significantly increase. On the other hand, increasing the PA content in the spinning dope decreased the water content of the PES hollow fiber mem-

branes. Permeation flux for oily wastewater treatment through the PES membranes decreased and TOC rejection increased by increasing PA concentration in spinning dope.

According to the results, PES hollow fiber membranes can be applied as an advanced method for treatment of the oily wastewaters. TOC rejection of the PES hollow fiber membranes was found to be more than 76% for the industrial oily wastewater. The results indicated that the PES hollow fiber membranes performed suitable TOC rejection (92.6%), high permeation flux (247.19 $L/m^2 \cdot h$).

Furthermore, Hermia's models were used for permeation flux decline prediction. Experimental results of permeation flux versus filtration time were compared to the Hermia fouling models. A comparison of the predicted permeation flux values and the experimental data shows that predictions are good enough for any experimental condition tested. It can be concluded that the complete pore blocking model fits worse to the experimental data than the other models considered in this work, and the intermediate blocking model fits accurately to experimental results. The reasonable agreement to experimental data corresponded to synthesized hollow fiber membranes to the cake layer formation model for all the experimental conditions tested. Also, permeation fluxes predicted by intermediate pore blocking models indicated good agreement with the experimental results.

REFERENCES

1. P. Canizares, F. Martınez, C. Jimenez, C. Saez and M. A. Rodrigo, *J. Hazard. Mater.*, **151**, 44 (2008).
2. K. H. Song and K. R. Lee, *Korean J. Chem. Eng.*, **24**, 116 (2007).
3. A. Salahi and T. Mohammadi, *Water Sci. Technol.*, **63**, 1476 (2011).
4. Q. Li, V. L. Snoeyink, B. J. Mariñas and C. Campos, *Water Res.*, **37**, 4863 (2003).
5. J. Kim, Z. Cai and M. M. Benjamin, *J. Membr. Sci.*, **310**, 356 (2008).
6. S. S. Madaeni, M. Rahimi and M. Abolhasani, *Korean J. Chem. Eng.*, **27**, 206 (2010).
7. M. Tomaszewska and S. Mozia, *Water Res.,* **36**, 4137 (2002).
8. H. Oh, M. Yu, S. Takizawa and S. Ohgaki, *Desalination*, **192**, 54 (2006).
9. J. H. Kweon, H. W. Hur, G. T. Seo, T. R. Jang, J. H. Park, K. Y. Choi and H. S. Kim, *Desalination*, **249**, 212 (2009).
10. Z. Ying and G. Ping, *Sep. Purif. Technol.*, **52**, 154 (2006).
11. Y. Matsuim, A. Yuasam and K. Ariga, *Water Res.*, **35**, 455 (2001).
12. F. Harrelkas, A. Azizi, A. Yaacoubi, A. Benhammou and M. N. Pons, *Desalination*, **235**, 330 (2009).
13. T. Suzuki, Y. Watanabe, G. Ozawa and S. Ikeda, *Desalination,* **117**, 119 (1998).
14. Q. Shi, Y. Su, S. Zhu, C. Li, Y. Zhao and Z. Jiang, *J. Membr. Sci.,* **303**, 204 (2007).
15. Z. M. Liu, Z. K. Xu, L. S. Wan and J. Wu, *J. Membr. Sci.*, **249**, 21 (2005).
16. V. Ghaffarian, S. M. Mousavi, M. Bahreini and H. Jalaei, *J. Ind. Eng. Chem.*, **20**, 1359 (2014).
17. M. A. Frommer and R. M. Messalem, *Ind. Eng. Chem. Prod. Res. Dev.*, **12**, 328 (1973).
18. N. Peng, N. Widjojo, P. Sukitpaneenit, M. M. Teoh, G. G. Lipscomb, T. S. Chung and J. Y. Lai, *Prog. Polym. Sci.*, **37**, 1401 (2012).
19. N. Vogrin, Č. Stropnik, V. Musil and M. Brumen, *J. Membr. Sci.*, **207**, 139 (2002).
20. H. Strathmann and K. Kock, *Desalination*, **21**, 241 (1977).
21. K. In-Chul and L. Kew-Ho, *J. Appl. Polym. Sci.*, **89**, 2562 (2003).
22. Q. Z. Zheng, P. Wang and Y. N. Yang, *J. Membr. Sci.,* **279**, 230 (2006).
23. T. Hui-An, R. Ruoh-Chyu, W. D. Ming and L. Juin-Yih, *J. Appl. Polym. Sci.*, **86**, 166 (2002).
24. J. Y. Lai, F. C. Lin, C. Ch. Wang and D. M. Wang, *J. Membr. Sci.,* **118**, 49 (1996).
25. H. J. Kim, R. K. Tyagi, A. E. Fouda and K. Ionasson, *J. Appl. Polym. Sci.*, **62**, 621 (1996).
26. H. Y. Niu, W. Z. Lang, Y. X. Liu and Y. J. Guo, *Fiber Polym.,* **14**, 1587 (2013).
27. B. Chakrabarty, A. K. Ghoshal and M. K. Purkait, *J. Membr. Sci.*, **315**, 36 (2008).
28. L. P. Zhu, L. Xu, B. K. Zhu, Y. X. Feng and Y. Y. Xu, *J. Membr. Sci.*, **294**, 196 (2007).
29. M. Amirilargani and T. Mohammadi, *Polym. Adv. Technol.*, **20**, 993 (2009).
30. I. M. Wienk, R. M. Boom, M. A. M. Beerlage, A. M. W. Bulte, C. A. Smolders and H. Strathmann, *J. Membr. Sci.*, **113**, 361 (1996).
31. A. Idris, A. F. Ismail, M. Y. Noordin and S. J. Shilton, *J. Membr. Sci.*, **205**, 223 (2002).
32. D. B. Jimenez, R. M. Narbaitz, T. Matsuura, G. Chowdhury, G. Pleizier and J. P. Santerre, *J. Membr. Sci.,* **231**, 209 (2004).
33. I. C. Kim and K. H. Lee, *J. Membr. Sci.*, **230**, 183 (2004).
34. E. Saljoughi, M. Sadrzadeh and T. Mohammadi, *J. Membr. Sci.*, **326**, 627 (2009).
35. M. Amirilargani, M. Sadrzadeh and T. Mohammadi, *J. Polym. Res.,* **17**, 363 (2010).
36. A. Salahi, T. Mohammadi, M. Nikbakht, M. Golshenasa and I. Noshadi, *Desal. Wat. Treat.*, **48**, 27 (2012).
37. T. Mohammadi, A. Salahi and M. Abbasi, *Desalination,* **251**, 153 (2010).
38. S. R. H. Abadi, M. R. Sebzari, M. Hemati, F. Rekabdar and T. Mohammadi, *Desalination*, **265**, 222 (2011).
39. APHA—American Public Health Association/American Water Works Association/Water Environment Federation, Standard Methods for the Examination of Water and Wastewater, 2001, 20th Ed., Washington, DC, USA (2001).
40. V. Laninovic, *Desalination,* **186**, 39 (2005).
41. J. F. Li, Z. L. Xu, H. Yang, C. P. Feng, J. H. Shi and J.-F. Li, *J. Appl. Polym. Sci.*, **107**, 4100 (2008).
42. M. Amirilargani, E. Saljoughi, T. Mohammadi and M. R. Moghbeli, *Polym. Eng. Sci.*, **50**, 885 (2010).
43. A. Rahimpour, S. S. Madaeni and Y. Mansourpanah, *J. Membr. Sci.*, **296**, 110 (2007).
44. S. S. Madaeni and S. Hoseini, *J. Polym. Res.*, **16**, 591 (2009).
45. D. M. Wang, F. C. Lin, T. T. Wu and J. Y. Lai, *J. Membr. Sci.,* **142**, 191 (1998).
46. H. Strathmann, K. Kock, P. Amar and R. W. Baker, *Desalination*, **16**, 179 (1975).
47. M. Amirilargani, E. Saljoughi and T. Mohammadi, *J. Appl. Polym. Sci.*, **115**, 504 (2010).
48. C. A. Smolders, A. J. Reuvers, R. M. Boom and I. M. Wienk, *J. Membr. Sci.*, **73**, 259 (1992).

49. N. A. Rahman, T. Solani and H. J. Matsuyama, *Appl. Polym. Sci.,* **108**, 3411 (2008).
50. J. H. Kim and K. H. Lee, *J. Membr. Sci.,* **138**, 153 (1998).
51. M. Sivakumar, R. Malaisamy, C. J. Sajitha, D. Mohan, V. Mohan and R. Rangarajan, *J. Membr. Sci.,* **169**, 215 (2000).
52. B. Chakrabarty, A. K. Ghoshal and M. K. Purkait, *J. Membr. Sci.*, **309**, 209 (2008).
53. J. Y. Lai, F. C. Lin, C. C. Wang and D. M. Wang, *J. Membr. Sci.*, **118**, 49 (1996).
54. W. L. Chou, D. G. Yu, M. C. Yang and C. H. Jou, *Sep. Purif. Technol.,* **57**, 209 (2007).
55. R. M. Boom, I. Wienk, T. V. D. Boomgaard and C. A. Smolders, *J. Membr. Sci.,* **73**, 277 (1992).
56. T. Mohammadi and E. Saljoughi, *Desalination*, **249**, 850 (2009).
57. E. Saljoughi, M. Amirilargani and T. Mohammadi, *J. Appl. Polym. Sci.,* **111**, 2537 (2009).
58. T. Mohammadi and E. Saljoughi, *Desalination*, **243**, 1 (2009).
59. M. Amirilargani and T. Mohammadi, *Sep. Sci. Technol.,* **44**, 3854 (2009).
60. T. H. Young and L. W. Chen, *J. Membr. Sci.,* **59**, 169 (1991).
61. J. Hermia, *Trans. Inst. Chem. Eng.*, **60**, 183 (1982).
62. M. C. V. Vela and S. Blanco, *Sep. Purif. Technol.*, **62**, 489 (2008).
63. S. M. Kumar and S. Roy, *Sep. Sci. Technol.*, **43**, 1034 (2008).
64. C. Xiaojun and K. H. Choo, *Environ. Eng. Res.*, **19**, 1 (2014).
65. A. Salahi, A. Gheshlaghi, T. Mohammadi and S. S. Madaeni, *Desalination*, **262**, 235 (2010).